



**HAL**  
open science

## Analysis of targeted phenolic ageing markers in Syrah red wines during bottle ageing: Influence of cork oxygen transfer rate

Luca Garcia, Elodie Martet, Lucas Suc, François Garcia, Cédric Saucier

### ► To cite this version:

Luca Garcia, Elodie Martet, Lucas Suc, François Garcia, Cédric Saucier. Analysis of targeted phenolic ageing markers in Syrah red wines during bottle ageing: Influence of cork oxygen transfer rate. Food Chemistry, 2024, 443, pp.138491. 10.1016/j.foodchem.2024.138491 . hal-04573473

**HAL Id: hal-04573473**

**<https://hal.inrae.fr/hal-04573473v1>**

Submitted on 22 Nov 2024

**HAL** is a multi-disciplinary open access archive for the deposit and dissemination of scientific research documents, whether they are published or not. The documents may come from teaching and research institutions in France or abroad, or from public or private research centers.

L'archive ouverte pluridisciplinaire **HAL**, est destinée au dépôt et à la diffusion de documents scientifiques de niveau recherche, publiés ou non, émanant des établissements d'enseignement et de recherche français ou étrangers, des laboratoires publics ou privés.



Distributed under a Creative Commons Attribution 4.0 International License



# Analysis of targeted phenolic ageing markers in Syrah red wines during bottle ageing: Influence of cork oxygen transfer rate

Luca Garcia, Elodie Martet, Lucas Suc, François Garcia, Cédric Saucier\*

SPO, Univ Montpellier, INRAE, Institut Agro, Montpellier, France

## ABSTRACT

A Syrah red wine ageing experiment was set up during 24-months and the influence of four micro-agglomerated corks were investigated. Specific phenolic ageing markers were selected and hemi-synthesized: vitisin B, malvidin-ethyl-catechin, and epicatechin-sulfonate. A targeted quantification method of these markers was then developed and validated by using ultra-high performance liquid chromatography - triple quadrupole mass spectrometry (UHPLC-QqQ-MS) operating in MRM (Multiple Reaction Monitoring). Results showed a significant decline in native grape polyphenol levels (anthocyanins, flavanols) as ageing progresses while pyranoanthocyanins, ethyl-linked pigments, and flavanol-sulfonates content increased. The cork oxygen transfer rate emerged as a pivotal factor and had significant effects on polyphenolic concentration evolution but had no significant impact on flavanol-sulfonate formation. These results provide valuable insights into the chemical evolution ongoing during wine ageing, accentuating the pivotal role of cork stopper selection in preserving wine quality over time.

## 1. Introduction

Polyphenols present in red wines are secondary metabolites that are extracted from grapes during winemaking process. These compounds play a crucial role in determining the wine sensory characteristics, including astringency and mouthfeel (Vidal et al., 2004). The color of red wine is also influenced by its phenolic composition, particularly by the presence of anthocyanins (Fulcrand et al., 2006). Additionally, there is a recognized positive correlation between the intensity of red wine color and its overall quality (Jackson et al., 1978). Hence, the phenolic composition emerges as a significant parameter in assessing the quality of red wine.

As a result of their inherent reactivity, the polyphenols become the primary substrates for transformative reactions during the ageing process of wine. A multitude of complex reactions takes place, leading to the modification and enhancement in the wine sensory properties (Tao et al., 2014). Indeed, wine ageing is an important stage in the production of high-quality red wine.

The primary transformation in red wine ageing is its colour evolution. The bright violet-red hue gradually moves towards a reddish-brown brick hue (Ribéreau-Gayon et al., 1998). This change in colour is mainly due to the decrease of native anthocyanins concentration (Alcalde-Eon et al., 2006). Over time, these anthocyanins are progressively and irreversibly replaced by more chemically stable pigments, particularly resistant to pH variations and decolorization caused by sulfur dioxide (Somers, 1971). The direct condensation of anthocyanins

and flavanols leads to the formation of polymeric pigments (Alcalde-Eon et al., 2006; Salas et al., 2004). Additionally, indirect condensation through aldehydes between flavanol and/or anthocyanin units can occur (Alcalde-Eon et al., 2006). Among the intermediate compounds involved, acetaldehyde has a significant importance. The condensation of anthocyanins and flavanols mediated by acetaldehyde results in the creation of new violet pigments (Pissarra et al., 2005), intensifying the color at the early stages of ageing, however, these pigments can be unstable under enological conditions (Escribano-Bailón et al., 2001).

In addition to indirect condensation, there is an additional evolutionary mechanism involving cycloaddition that includes acetaldehyde, pyruvic acid, vinylphenol, or vinylcatechol (Bakker & Timberlake, 1997; Mateus et al., 2001). This particular mechanism leads to a new group of pigments derived from anthocyanins, known as pyranoanthocyanins, which have a pronounced hypsochromic effect, leading to an increased orange hue (Bakker & Timberlake, 1997). While acetaldehyde and pyruvic acid are originally occurring through yeast metabolism, aldehyde concentrations can also significantly increase in wine due to oxygen exposure during ageing (Wildenradt & Singleton, 1974). This could lead to an increase in the concentration of polyphenols derivatives such as ethyl-linked oligomers and pyranoanthocyanins. In addition, these new anthocyanin-derived pigments formed during ageing exhibit more stable structures that may stabilize wine colour (Echave et al., 2021).

During the ageing process of red wine, changes in mouthfeel properties become apparent as a reduction in both astringency and bitterness may occur. These changes can be attributed to the occurrence of

\* Corresponding author.

E-mail address: [cedric.saucier@umontpellier.fr](mailto:cedric.saucier@umontpellier.fr) (C. Saucier).

oxidative and non-oxidative polymerizations (Echave et al., 2021), as well as the precipitation of phenolic compounds like tannins, particularly during bottle ageing. Some studies (Arapitsas et al., 2014; Ma et al., 2018) suggest that tannins might undergo reaction with sulfur dioxide, resulting in the formation of flavanols sulfonates. This reaction is thought to potentially play a role in the decrease of astringency that is commonly observed during red wines ageing.

Typically, high-quality red wines benefit from a period of ageing in the bottle before they are consumed, allowing them to reach an optimal state (Gambuti et al., 2013). Two important factors will influence the wine shelf life: the total packaged oxygen (*i.e.* dissolved and head-space oxygen) in the bottle and the supply of oxygen through the bottle stopper.

The first factor is the initial oxygen release (OIR), which refers to the oxygen trapped within the microstructure of the cork which is expelled when the cork is compressed during the bottling process. The second factor is the oxygen transfer rate (OTR) of the closure, which represents the amount of oxygen that passes through the closure during ageing (Pons et al., 2022). A study indicated that the OTR through the cork may be the primary factor contributing to the differential evolution of the wine over time (Boulton, 2005). Previous research has demonstrated the impact of OTR on the evolution of polyphenols: the degradation of anthocyanins and flavan-3-ol monomers was shown to be significantly influenced by OTR (Wirth et al., 2010). Therefore, the concentration of these latter decrease during ageing and also with OTR increase (Giuffrida de Esteban et al., 2019; Wirth et al., 2012). Additionally, OTR affect the increase of large polymeric pigments during wine ageing (Giuffrida de Esteban et al., 2019). Furthermore, OTR was also identified as a factor influencing the formation of specific pigment derivatives, such as vitisin A, vitisin B, (Wirth et al., 2010) and other pyranoanthocyanins during the initial months of ageing (Alcalde-Eon et al., 2006). In addition, during the formation of pyranoanthocyanins, a final oxidation reaction is necessary to allow the re-aromatisation of pyranic D ring to form vitisin-like pigments (de Freitas and Mateus, 2011).

Concerning colour evolution, previous research demonstrated that an increase in OTR led to a more intense orange tint (Wirth et al., 2010). Nevertheless, the findings are contrasted concerning colour intensity. Some studies showed a significant correlation between OTR and colour intensity (Wirth et al., 2010) while others have found no discernible influence (Gambuti et al., 2013).

As polyphenols are major substrates for various chemical reactions and are largely responsible for organoleptic changes during the ageing of red wine, the main objectives of this article are:

- Develop a UHPLC-Qq-MS method to quantify selected polyphenols during Syrah red wine ageing.
- Study the kinetics of these polyphenols during Syrah wine ageing.
- Study the influence of microagglomerated cork oxygen transfer rate on these kinetics.

## 2. Materials and methods

### 2.1. Reagents, solvents and standards

Onen chloride, catechin, epicatechin, epigallocatechin, epicatechin-3-O-gallate and procyanidins B1, B2 and B3 were obtained from Extrasynthese (Genay, France). Sodium metabisulfite, phloroglucinol and ammonium acetate were obtained from Sigma-Aldrich (Saint-Quentin Fallavier, France). Formic acid was obtained from Carlo Erba Reagents (Peypin, France). Acetaldehyde and vinyloxytrimethylsilane were obtained from Honeywell Fluka (Illkirch, France). LC – MS-grade methanol, acetonitrile, water, trifluoroacetic acid and formic acid were purchased from Biosolve (Dieuze, France).

### 2.2. Wine samples and stoppers

Six red wines samples (100 % Syrah) were obtained from different wineries from Côtes du Rhône and Languedoc-Roussillon area. All the wines were in the maturation phase in tank or oak barrel and close to bottling. The name, denomination of origin, vintage and ageing type are summarized in Table 1. Four different microagglomerated cork stopper were provided by DIAM Bouchage (Céret, France), each measuring  $44 \pm 0.2 \times 24 \pm 0.1$  mm in dimensions. The oxygen transfer rates (OTR) and oxygen initial rates (OIR) data were provided by the supplier (Table 1).

The six wines were bottled following conventional winemaking methods. Free SO<sub>2</sub> levels were adjusted up to 30 mg.L<sup>-1</sup> before bottling. Empty 0.75 L Bordelaise bottles were manually placed and inerted with nitrogen on the filling machine. After filling the bottles with 0.75 L of wine, cork stopper types were manually inserted using a vacuum corker in a random order.

After bottling, the dissolved oxygen concentrations for each wine were measured by an external laboratory BO Solutions (Rivesaltes, France). The results are given in Table S1 (Supplementary data). No statistical differences were observed in terms of dissolved oxygen in the samples after bottling.

All the biological triplicate combination of bottles and corks were aged during 0, 6, 12 and 24 (t0, t6, t12 and t24) months at 17 °C. Therefore, at each kinetic point, 72 bottles were opened (6 wines x 4 cork x 3 biological replicate). A total of 252 bottles were opened during this study.

Subsequently, each opened bottle was aliquoted into 2 mL plastic vials under argon gas and promptly frozen at –80 °C. For each further analysis, biological triplicate (3 vials from three different bottles) were used.

### 2.3. Enological parameters

The following enological parameters were measured for each wine after bottling by Laboratoires Dubernet (Narbonne, France): Alcoholic percentage was determined by Fourier transformed infrared spectroscopy (FTIR) (WineScan, FOSS France, Nanterre, France), total acidity by titration (OIV-MA-AS313-01), volatile acidity, free SO<sub>2</sub> and total SO<sub>2</sub> were determined by automatic colorimetric method using sequential analysers, pH by potentiometric method, iron and copper were quantified by microwave-induced plasma atomic emission spectrometry (MP-AES) (Agilent France) (OIV-OENO 637–2021).

### 2.4. Synthesis of malvidin-3-O-glucoside-8-ethyl-catechin (malvidin-ethyl-catechin)

The synthesis of malvidin-ethyl-catechin (1) was adapted from Pisara et al. (Pissarra et al., 2005). In a round bottom flask, 1 equivalent of malvidin-3-O-glucoside and 5 equivalents of (+)-catechin were dissolved in a 12 % hydroalcoholic solution (pH adjusted at 1.5 with 0.1 N HCl), then 20 equivalents of acetaldehyde were added. The mixture was

**Table 1**  
Characteristics of the red wines samples and corks.

Code	Denomination of origin	Vintage	Ageing
CR1	Côtes du Rhone	2020	Tank
LR1	Languedoc-Roussillon	2019	Oak barrel
LR2	Languedoc-Roussillon	2019	Oak barrel
LR3	Languedoc-Roussillon	2019	Tank
LR4	Languedoc-Roussillon	2019	Oak barrel
CR2	Côtes du Rhone	2019	Oak barrel
Code	Type	OIR (mg)	OTR (mg/year)
DIAM 1 (D1)	Microagglomerated cork	0.77 ± 0.03	0.3 ± 0.1
DIAM 2 (D2)	Microagglomerated cork	1.72 ± 0.25	0.9 ± 0.1
DIAM 3 (D3)	Microagglomerated cork	1.76 ± 0.15	1.1 ± 0.1
DIAM 4 (D4)	Microagglomerated cork	2.19 ± 0.13	1.8 ± 0.4

heated under reflux protected from light at 35 °C and stirred at 400 rpm during 4 h. The resulting reaction medium was applied on a low-pressure reverse phase silica C18 column chromatography and washed with 1 % formic acid water in order to remove the unreacted acetaldehyde. Another elution was performed with 1 % formic acid MeOH/H<sub>2</sub>O solution (30/70; v/v) to yield a violet-coloured fraction. The final isolation of (**1**) was performed by low pressure TSK Toyopearl HW-40(S) gel column chromatography with 20 % methanol acidified with 1 % formic acid. Finally, to remove formic acid a solid-phase extraction (SPE) step was used: The resulting fractions were deposited on a 5g C<sub>18</sub> cartridge (Supelco, St Quentin Fallavier, France) conditioned with 50 mL of MeOH followed by 50 mL of H<sub>2</sub>O. After application of the fractions, the column was washed with 50 mL of water. The dimers were then eluted with 5 mL of methanol. Then, methanol was evaporated through rotary evaporation under vacuum and the isolated compound was redissolved in minimum amount of water and freeze-dried to give (**1**) as a purple powder.

### 2.5. Synthesis of vitisin B

The synthesis of pyranoanthocyanin vitisin B (**2**) was performed as described by Oliveira et al. (Oliveira et al., 2009). Briefly, in a round bottom flask 1 equivalent of malvidin-3-O-glucoside was dissolved in a 12 % hydroalcoholic solution (pH adjusted at 2.5 with 0.1 N HCl), then 200 equivalents of vinyloxy-trimethylsilane were added dropwise. The maximum amount of compound (**2**) was reached after 3 h. The mixture was left to react at room temperature with continuous agitation at 400 rpm. Then, the reaction was stopped by solid phase extraction (SPE) using 1 g of C18 cartridge previously conditioned with 10 mL of methanol following by 10 mL of water. After application of the crude mixture, the cartridge was washed with 10 mL of water in order to neutralize the pH and to remove the unreacted vinyloxy-trimethylsilane and the resulting pigments were isolated with methanol, concentrated and freeze-dried. Finally, isolation of a (**2**) was performed by low pressure TSK Toyopearl gel HW-40(S) column chromatography with 20 % methanol in water. Then, methanol was removed by rotary evaporation under partial vacuum and the isolated compound was freeze-dried to give (**2**) as an orange powder.

### 2.6. Synthesis of epicatechin-SO<sub>3</sub>H

Epicatechin-SO<sub>3</sub>H (**3**) was synthesized as described by Ma et al. (Ma et al., 2018). Briefly, in a round bottom flask, 1 g.L<sup>-1</sup> of white grape seed tannin extract (Union des distilleries de la Méditerranée) in methanol was treated with 10 g.L<sup>-1</sup> SO<sub>2</sub> solution in H<sub>2</sub>O (obtained by dissolving sodium metabisulfite (Na<sub>2</sub>S<sub>2</sub>O<sub>5</sub>)) and pH was adjusted at 2.0 with HCl. The crude was then heated at 50 °C under reflux using an oil bath overnight. Then, the methanol was removed under rotary evaporation under partial vacuum. Epicatechin-SO<sub>3</sub>H was then isolated using a semi-preparative Bio-Rad NGC 10 medium-pressure chromatography system (Bio-Rad, Hercules, CA, USA) equipped with a reversed-phase C18 Simply column 150 g (40–60 μm) (AIT, Cormeilles-en-Parisis, France). The purification was performed at a constant flow rate of 20 mL.min<sup>-1</sup>. The binary mobile phase consisted of water (solvent A) and acetonitrile (solvent B) and the elution conditions were: 0 % B for 20 min; 0 – 15 % B in 15 min; 15 – 95 % B in 2 min; 95 % B for 10 min, 95 – 0 % B in 1 min, finally 0 % B for 10 min. Fractions containing (**3**) were combined, reduced under pressure and freeze-dried to give (**3**) as a white powder.

### 2.7. UPLC-DAD-MS for reaction monitoring

The reactions and the purifications were monitored using two UPLC-DAD-MS systems. The first one was a reversed-phase Ultra-High-Performance Liquid Chromatography coupled to Mass Spectrometry (UHPLC-MS) system. The liquid chromatography system was an Acquity UPLC (Waters, Milford, MA, USA) equipped with a photodiode array

detector. An Acquity UPLC HSS T3 column (1.8 μm, 2.1 × 100 mm) was used. The column temperature was 30 °C. The binary mobile phase consisted of 0.1 % trifluoroacetic acid in water (solvent A) and acetonitrile (solvent B). The separation was performed at a constant flow rate of 0.25 mL.min<sup>-1</sup>, using the following gradient: 10 – 18 % B in 1 min; 18 – 40 % B in 9 min; 40 – 90 % B in 0.5 min; 90 % B for 1.5 min; 90 – 10 % B in 0.5 min; finally 10 % B for 1.5 min. The injection volume was 7.5 μL. The mass spectrometer was a Waters Acquity QDa electrospray ionization (ESI) simple quadrupole (Waters, Milford, MA, USA). The capillary voltage was set at 0.8 kV. The mass spectra were acquired over a mass range of 200–900 Th in the positive ion mode.

The second one used for a rapid verification during the semi-preparative purification steps was the same chromatographic system described previously. The column was heated at 38 °C. The binary mobile phase consisted of water (solvent A) and 80 % acetonitrile in water (solvent B) both acidified with 1 % formic acid. The separation was performed at a constant flow rate of 0.55 mL.min<sup>-1</sup>, using the following gradient: 8–11 % B in 2 min; 11 % B for 8 min; 11–25 % B in 15 min; 25–55 % B in 5 min; 55–99 % B in 1 min; 99 % B for 4 min; 99–8 % B in 1 min; 8 % B for 4 min. The injection volume was 2 μL. The mass spectrometer was a Waters Acquity QDa electrospray ionization (ESI) simple quadrupole (Waters, Milford, MA, USA). The mass spectrometer was a Bruker amaZon X electrospray ionization (ESI) ion trap (Bruker Daltonics, Bremen, Germany). The capillary voltage was set at – 5.5 kV. The mass spectra were acquired over a mass range of 50–1500 Th in the positive ion mode.

### 2.8. NMR characterization of synthesized compounds

<sup>1</sup>H NMR spectra were recorded at 25 °C using a 400 MHz Bruker Advance NEO spectrometer operating at 400.17 MHz for 1H equipped with a 5 mm BBI probe. The sample was dissolved in DMSO-d<sub>6</sub> /TFA (9/1). NMR data were processed and analyzed using both TopSpin 4.0 (Bruker) and MestReNova 14.3.3 software (Mestrelab Research, Spain). Quantification was performed using ERETIC2 method. All spectra were referenced to the solvent dmsO-d<sub>6</sub> signals (1H residual signal at 2.50 ppm).

### 2.9. Electrochemical characterization of polyphenols standards

Electrochemical characterization of standard was performed by cyclic voltammetry. Polyphenols standards were prepared in model wine (ethanol 12 % (v/v), 33 mmol.L<sup>-1</sup> tartaric acid and pH 3.6 adjusted with 1 mol.L<sup>-1</sup> NaOH) at 0.1 mM for catechin, epicatechin, epicatechin-SO<sub>3</sub>H, malvidin-3-O-glucoside, vitisin B and 0.05 mM for malvidin-ethylcatechin. Then, 200 μL of standard solution were dropped on the electrode surface. The measurements were performed with a scan rate of 100 mV.s<sup>-1</sup> in the range of – 0.2 V to 0.3 V (vs. Ag(s)) except for malvidin-3-O-glucoside and vitisin B in the range of – 0.2 V to 0.8 V. A 4 mm diameter single-walled carbon nanotubes-modified screen-printed carbon electrode SWCNTs-SPCE (Dropsens, Oviedo, Spain) in a three-electrode configuration (carbon counter electrode and silver reference electrode) was used. The experiments were performed on a potentiostat/galvanostat (Autolab PGSTAT 302 N) using software Nova 2.1.5 (Metrohm, Herisau, Switzerland) in triplicate.

### 2.10. UHPLC-DAD analysis of tannins

The content of flavanols was investigated through acid-catalyzed depolymerisation of tannins in the presence of phloroglucinol, following the methodology described by Garcia et al. (Garcia et al., 2023). First, 400 μL of a red wine sample were dried in a centrifugal solvent evaporator (Genevac, Ipswich, UK). The resulting residue was then dissolved in 600 μL of a solution containing 50 g.L<sup>-1</sup> phloroglucinol and 10 g.L<sup>-1</sup> ascorbic acid in methanol-HCl (0.2 M). The reaction was conducted at 50 °C for 20 min and, afterwards, 600 μL of a 200 mM



ammonium acetate solution was added to quench the reaction. The sample was centrifuged at 12,000 rpm for 10 min and the supernatant was injected (7.5  $\mu\text{L}$ ) into the same chromatographic apparatus mentioned in section 2.7 equipped with a reversed phase UPLC Acquity UPLC BEH C18 column (50 mm length, 2.1 mm internal diameter, 1.7  $\mu\text{m}$  particle size) from Waters.

The chromatographic method employed was a binary gradient using mobile phase A (0.1 % v/v aqueous trifluoroacetic acid) and mobile phase B (acetonitrile). The elution process, at a flow rate of 0.45 mL  $\text{min}^{-1}$ , followed the pattern: 2 % B at 0 min, 2–6 % B from 0 to 10 min, 6–20 % B from 10 to 16 min, 20–99 % B at 16 to 16.1 min (isocratic), 99 % B at 16.1 to 18 min (isocratic), 99–2 % B from 18 to 18.1 min, and finally, isocratic with 2 % B from 18.1 to 22 min. The column temperature was maintained at 40 °C and detection of eluting peaks was done at 280 nm. This analysis allowed to determine the type and relative proportions of terminal and extension units of tannins. To quantify the results, an external catechin calibration curve was employed, and the concentrations of epicatechin, epigallocatechin and epicatechin-3-O-gallate were quantified their respective response factors relative to catechin (Garcia et al., 2023).

### 2.11. UHPLC-DAD analysis of monomeric anthocyanins

The quantification of monomeric anthocyanins was performed as described by Garcia et al. (Garcia et al., 2023). Wines samples were directly injected (7.5  $\mu\text{L}$ ) after a filtration on a 0.45  $\mu\text{m}$  PTFE filter (Macherey-Nagel, Düren, Germany) into the same chromatographic apparatus mentioned in section 2.10. The method used was a binary gradient with mobile phase A (0.1% v/v aqueous trifluoroacetic acid) and mobile phase B (acetonitrile). The column temperature was set at 50 °C. The 40 min elution method at flow 0.25 mL  $\text{min}^{-1}$  was 1 % B (0 min), 1–8.8 % (0–5 min) B, 8,8–20.6 % (5–30 min) B, 20.6–96 % (30–30.5 min) B, isocratic with 96 % B (30.5–34 min), 96–1 % (34–34.1 min) B and isocratic with 1 % B (34.1–40 min). The detection was monitored at 520 nm with a photodiode array detector (PDA).

External malvidin-3-O-glucoside calibration curve was used. Results were expressed as mg malvidin-3-O-glucoside equivalent (M3G eq)  $\text{L}^{-1}$ .

### 2.12. UHPLC-QqQ-MS analysis of polyphenols

#### 2.12.1. Analytical conditions

UHPLC-QqQ-MS analyses were carried out using a 1290 Infinity II UHPLC (Agilent Technologies, Santa Clara, CA, USA) hyphenated to a 6470B Agilent Triple Quadrupole. Analytes were separated with a reversed phase UPLC Acquity UPLC BEH C18 column (100 mm length, 2.1 mm internal diameter, 1.7  $\mu\text{m}$  particle size) (Waters, Saint-Quentin-Yvelines, Franc). The chromatographic method was adapted from Lambert et al. (Lambert et al., 2015) with modifications. The method was a binary gradient with mobile phase A (1 % v/v aqueous formic acid) and mobile phase B (0.1 % v/v formic acid in methanol). The

column temperature was set at 40 °C. The flow rate was set at 0.5 mL  $\text{min}^{-1}$ . The gradient was isocratic 1 % B (2 min), 1 – 10 % B (2–10 min), 10–28 % B (10–20 min), 28–45 % B (20–24 min), 45–99 % B (24–25.5 min), isocratic with 99 % B (25.5 – 30.5 min), 99–1 % B (30.5–31 min) and isocratic with 1 % B (31–34 min). Source parameters were optimized with Source and iFunnel Optimizer software 10.1 (Agilent) as follows: gas temperature at 230 °C, gas flow at 4 L  $\text{min}^{-1}$ , nebulizer at 55 psi, sheath gas temperature at 400 °C, sheath gas flow at 11 L  $\text{min}^{-1}$ , capillary voltage at 3000 V in positive mode, nozzle voltage at 0 V and positive Delta EMV at 200 V.

Ionization was carried out using positive electrospray (ESI + ) and detection was made using Multiple Reaction Monitoring (MRM). Quantification and qualification transitions were optimized with Optimizer 10.1 software (Agilent) by direct flow injection analysis of polyphenols solution and described in Table 2 and Table S2 (Supplementary data).

#### 2.12.2. Sample preparation and calibration

Red wines samples were centrifuged at 10,000 rpm during 10 min in order to remove solid particles. Then, 100  $\mu\text{L}$  was diluted ten times with 900  $\mu\text{L}$  model wine solution (ethanol 12 % (v/v), 33 mmol  $\text{L}^{-1}$  tartaric acid and pH 3.6 adjusted with 1 mol  $\text{L}^{-1}$  NaOH) and 10  $\mu\text{L}$  of a 250 mg  $\text{L}^{-1}$  solution of chlorogenic acid in methanol/ $\text{H}_2\text{O}$  20/80 (v/v) was added as internal standard before analysis.

As quantification by this method was subjected to matrix effects (see part 3.2), it was therefore not possible to quantify in a model matrix and calibration curves for each compound had to be prepared within the particular matrix under analysis. In practical terms, calibration ranges (as outlined in Table 2) were prepared by diluting a mixed solution of polyphenols prepared in methanol/ $\text{H}_2\text{O}$  20/80 (v/v) directly in the initial, non-aged wine (t0) for each type of wines. This calibrated range allowed the quantification of polyphenols in all wine samples.

#### 2.12.3. Validation

To validate the analytical method, several parameters were calculated before quantifying the wine samples: linearity, accuracy, repeatability, limit of detection (LOD) and limit of quantification (LOQ).

Matrix effect was measured by comparing the signal obtained in a model wine and in two Syrah red wines samples (RW<sub>1</sub> and RW<sub>2</sub>) spiked with a solution of mixed polyphenols at the same level of concentration in triplicate. Then, the matrix effect was evaluated by calculating the Z-score parameter for each molecule. If the Z-score is inferior to 2, it can be concluded that there was no matrix effect between model and real wine samples (Roland & Schneider, 2015).

Linearity was calculated by spiking two Syrah red wines samples at six concentrations (n = 3) for all polyphenols. Standard calibration curves were obtained from unweighted least-squares linear regression analysis of the data. The slope and intercept of the calibration graphs were determined through linear regression of the peak areas versus concentration plot. Individual peak areas were then interpolated on the

**Table 2**

List of quantified compounds, MRM parameters and calibration ranges.

Molecules	Ion Mode	Transition of quantification	Transition of qualification		Retention time (min)	Calibration (mg $\text{L}^{-1}$ )
Catechin	+	291→139	291→147	291→123	8.10	0.48–16.7
Epicatechin	+	291→139	291→147	291→123	12.86	0.48–16.7
Epigallocatechin	+	307→139	307→195	307→163	8.05	0.48–16.7
Epicatechin-3-O-gallate	+	443→123	443→273	443→139	16.33	0.48–16.7
Dimer B1	+	579→127	579→139	579→123	7.80	0.48–16.7
Dimer B2	+	579→127	579→139	579→123	11.20	0.48–16.7
Dimer B3	+	579→127	579→139	579→123	6.80	0.48–16.7
Dimer B4	+	579→127	579→139	579→123	9.05	0.48–16.7
Malvidin-3-O-glucoside	+	493→331	493→315	493→287	17.85	0.48–16.7
Epicatechin-SO3H	+	371→127	371→289	371→135	1.40	0.24–8.3
Vitisin B	+	517→355	517→339	517→266	19.62	0.24–8.3
Vitisin A	+	561→399	561→383		20.45	As equivalent of vitisin B
Malvidin-ethyl-catechin (2 isomers)	+	809→357	809→341	809→115	21.86/22.32	0.24–8.3

calibration graphs to determine the back calculated concentrations. The quality of fit was determined using back-calculated-to-nominal concentrations and the F-test was used to confirm the linearity of the method.

Accuracy and repeatability were measured by spiking two Syrah red wines samples at three different levels ( $n = 5$ ) for each compound and were expressed as the recovery and mean RSD (%), respectively.

The LOD and LOQ were calculated for each compound for a signal to noise (S/N) ratio equal to 3 and 10, respectively ( $n = 5$ ).

### 2.13. Statistical analysis

The ANOVA tests were performed using XLSTAT software (Addinsoft version 19.02, Paris, France). Tukey test was carried out and when  $p$ -values were  $< 0.05$  the data were considered as statistically significant. All analyses, experiments and tests were performed in triplicate.

## 3. Results and discussion

### 3.1. Choice, hemisynthesis and electrochemical characterization of polyphenols standards

Three key molecules that represent different families of polyphenols formed during wine ageing were chosen based on previous studies (Table 3). These molecules were:

- Malvidin-ethyl-catechin: This compound belongs to the ethyl-linked pigments family and is formed through the condensation of acetaldehyde with malvidin-3-O-glucoside and catechin (Pissarra et al., 2005).
- Vitisin B: This molecule is part of the pyranoanthocyanins family and results from the reaction between malvidin-3-O-glucoside and acetaldehyde (Mateus et al., 2001).

- Epicatechin-SO<sub>3</sub>H: Representing the flavanol sulfonate family, this compound is the product of sulfonation by SO<sub>2</sub> of proanthocyanins (Ma et al., 2018).

After synthesis, these markers were characterized and quantified by H<sup>1</sup> NMR in order to confirm their structure and purity (see spectra in supplementary data, Figure S1 and S2).

Furthermore, to investigate the redox properties of the hemi-synthesized ageing compounds and compare them with “native” grape phenolic compounds, the formal potential ( $E'_0$ ) of each molecule was determined using cyclic voltammetry with the following formula (1):

$$E'_0 = \frac{E_{pa} + E_{pc}}{2} \quad (1)$$

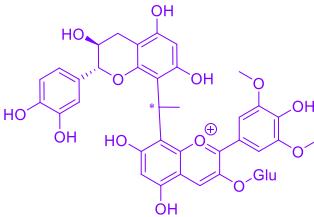
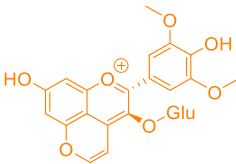
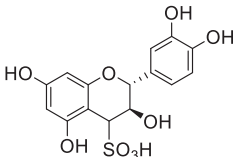
Where  $E_{pa}$  is the anodic peak potential and  $E_{pc}$  is the cathodic peak potential (for malvidin-3-O-glucoside and vitisin B, the oxidation reaction at the electrode was irreversible *i.e.* without return cathodic peak and  $E_{pc}$  was substituted by the potential at half the anodic peak height  $\frac{E_{pa}}{2}$ ).

This measurement allowed for the quantification of the reducing power of phenolic antioxidants: more the formal potential is low and more the reduction property is important. The results for catechin, epicatechin, malvidin-3-O-glucoside, epicatechin-SO<sub>3</sub>H, vitisin B and malvidin-ethyl-catechin are given in the table S3 (Supplementary data).

There is a tendency for potential values to increase in the following order: epicatechin-SO<sub>3</sub>H (105.8 mV) < epicatechin (110.8 mV) < malvidin-ethyl-catechin (111.1 mV) < catechin (117.2 mV) < malvidin-3-O-glucoside (358.9 mV) < vitisin B (383.3 mV). This classification highlights the diverse oxidation potentials exhibited by these compounds, which are influenced by their respective chemical reactivity and structural properties.

The presence of a methoxy group adjacent to the phenol group, for anthocyanins and derived pigments, diminished the reducing capacity of the molecules. Additionally, for vitisin B, it was shown that the formation of a fourth D ring involving the hydroxyl group at C5 and the C4

**Table 3**  
Family and structure of synthesized ageing markers.

Family of ageing markers	Molecules	Structure	Purity by H <sup>1</sup> NMR (ERETIC2)
Ethyl linked pigments	Malvidin-ethyl-catechin		77.6 %
Pyranoanthocyanins	Vitisin B		73.2 %
Flavanols-sulfonates	Epicatechin-SO <sub>3</sub> H		83.0 %

of the anthocyanin heterocycle may reduce its ability to capture electrons (Tománková et al., 2016).

### 3.2. Analytical validation of UHPLC-MS/MS method

In order to ensure reliable outcomes, the analytical method was validated following the recommendations of the International Organization of Vine and Wine (OIV-MA-AS1-12). The validation parameters are shown in Table 4.

The first parameter assessed during the validation process was the matrix effect, which gauges the method specificity. This involved spiking at two different concentrations a mixed solution of the 11 compounds in three different matrices: a model wine and two Shiraz wines. The matrix effect was assessed by calculating the z-score parameter, as described in the literature (Roland & Schneider, 2015).

As shown in Tables S4 (Supplementary data), epicatechin-3-O-gallate, procyanidins dimer B1, B2 and epicatechin-SO<sub>3</sub>H exhibited no matrix effect, as their z-scores were below 2 for both matrices. However, the remaining compounds showed z-scores ranging from 2.011 to 6.506, indicating the need for calibration in a red wine matrix instead of model wine solution.

To avoid matrix effects, we chose the standard addition method, which involves adding the calibration standard solutions directly to the sample to be analysed. Calibration curves for each compound were then prepared directly in the initial non-aged sample (t<sub>0</sub>) for each of the six wines with addition concentrations ranging from 0.24 to 16.7 mg/L for each analyte. These calibration curves were then used to quantify the molecular targets for each of the associated wines. The quantification process involved UHPLC-MS/MS analysis in multiple reaction monitoring mode (MRM). The peak area for quantifier ions were plotted against the corresponding concentration to generate these curves.

Subsequently, the individual peak areas were then interpolated on the calibration graphs to calculate the back-calculated concentrations. The linearity of the method was assessed by evaluating the quality of fit through back-calculated-to-nominal concentrations and employing the F-test for the confirmation of the method linearity. The linear model was proved to be suitable for all analytes as the R<sup>2</sup> values for each polyphenol were above 0.99.

Accuracy was determined by adding known amounts of polyphenols mix to two different wines at three concentration levels (0.45, 2.1 and 4.5 mg.L<sup>-1</sup>). Control samples (non-spiked wines) were also analysed to differentiate between natural and spiked quantities of polyphenols. By comparing the calculated quantity to the theoretical spiked amount, the accuracy of the method was evaluated. The results showed accuracy ranging from 96.6 % to 108.8 % for all analytes under the given conditions, ensuring reliable outcomes (Table 4). These values are in line with the OIV resolutions, where an accuracy range of 80 % to 120 % is considered satisfactory.

Repeatability was examined by spiking two Shiraz wines at three different concentrations (0.45, 2.1 and 4.5 mg.L<sup>-1</sup>) on the same day. The

relative standard deviation (RSD%) was calculated and ranged from 3.0 % to 6.8 % for all analytes, which was deemed acceptable. Indeed, OIV recommends a repeatability value below 20 %.

At last, limits of detection (LOD) and quantification (LOQ) were calculated using a signal-to-noise ratio of 3 and 10, respectively. For all compounds, the LOD ranged from 0.3 to 26.4 µg.L<sup>-1</sup>, while the LOQ ranged from 0.9 to 88 µg.L<sup>-1</sup>. These values showed the high sensitivity of our method for quantification, with limits well below the concentrations classically found in wines (Section 3.3).

### 3.3. Initial characterization of red wine samples

First, the six Syrah red wines were characterized just after bottling in term of enological parameters and polyphenolic composition as detailed in Table S5 (Supplementary data).

Volatile acidity levels ranged from 0.31 to 0.67 g.L<sup>-1</sup> H<sub>2</sub>SO<sub>4</sub>, which were all lower than the authorized limit of 0.98 g.L<sup>-1</sup> H<sub>2</sub>SO<sub>4</sub>, according to OIV resolutions. In term of total acidity, the levels ranged between 2.72 and 3.41 g.L<sup>-1</sup> of tartaric acid while pH ranged from 3.64 to 3.97. In addition, % of ethanol ranged from 12.95 to 16.16 %. All these parameters are typical of red wines from the warm climate of south of France. The levels of free SO<sub>2</sub> were adjusted before bottling around 30 mg.L<sup>-1</sup> for all wines. Copper concentration ranged from 0.34 to 0.53 mg.L<sup>-1</sup> and iron concentration from 0.70 to 3.13 mg.L<sup>-1</sup> so there were no risk of unstable metal haze precipitations in these wines since all levels were inferior to 10 mg.L<sup>-1</sup> and 1 mg.L<sup>-1</sup> respectively.

Concerning polyphenolic compounds, after bottling, the concentrations of flavan-3-ol monomers (sum of catechin, epicatechin, epigallocatechin and epicatechin-3-O-gallate) ranged between 102.65 and 242.90 mg.L<sup>-1</sup> with majority of catechin in all of the six wines. These concentrations were classical for young Syrah red wine (Landraut et al., 2001) with the higher concentration found for the youngest red wine (CR1).

Moreover, the concentrations of flavan-3-ol dimers (sum of B1, B2, B3 and B4) ranged between 75.29 and 156.90 mg.L<sup>-1</sup> and were in agreement with previous results for a red wine (Landraut et al., 2001; Quagliari et al., 2017) with higher concentration for procyanidins dimer B1 (epicatechin-4-8-catechin) for all the wines. For the total flavanols determined after acid depolymerization in presence of phloroglucinol, the concentration ranged from 1.29 to 3.13 g.L<sup>-1</sup>. Concentrations of monomeric anthocyanins in the wine studied ranged from 111.91 to 352.41 mg.L<sup>-1</sup> in accordance with previous studies (García-Beneytez et al., 2003; Revilla et al., 2001). Closer examination of the anthocyanin profiles revealed that the proportion of anthocyanins mono-glucosides were between 64.4 and 72.3 % of total monomeric anthocyanins. On the other side, their esterified forms (acetylated and coumaroylated) were less concentrated and represented between 17.4 and 24.1 % for acetylated anthocyanins and 9.05 and 14.14 % for coumaroylated anthocyanins. However, malvidin-3-glucoside derivatives (esterified or not) were the most abundant monomeric anthocyanin and represented

**Table 4**

Analytical performances for the UHPLC-MS/MS method (linearity (R<sup>2</sup>); accuracy; repeatability; LOD: limit of detection and LOQ: limit of quantification). Mean value ± standard deviation.

Molecules	Linearity (R <sup>2</sup> )	Accuracy (%)	Repeatability (%)	LOD (µg.L <sup>-1</sup> )	LOQ (µg.L <sup>-1</sup> )
Catechin	0.9958 ± 0.003	108.8 ± 6.5	6.8 ± 3.2	8.40	27.90
Epicatechin	0.9924 ± 0.0016	102.7 ± 6.8	6.2 ± 3.2	8.50	28.50
Epigallocatechin	0.9951 ± 0.0028	104.6 ± 8.6	3.4 ± 2.0	7.80	26.10
Epicatechin-3-O-gallate	0.9954 ± 0.0022	96.6 ± 7.6	3.6 ± 1.1	5.00	16.70
Dimer B1	0.9964 ± 0.0021	102.9 ± 5.5	6.5 ± 2.0	11.10	36.80
Dimer B2	0.9969 ± 0.0017	102.0 ± 6.6	6.1 ± 2.8	8.40	28.10
Dimer B3	0.9984 ± 0.0010	98.0 ± 8.0	3.8 ± 2.9	26.40	88.00
Malvidin-3-O-glu	0.9983 ± 0.0008	99.7 ± 6.2	6.1 ± 2.6	6.80	22.70
Epicatechin-SO <sub>3</sub> H	0.999 ± 0.0008	99.3 ± 4.2	4.5 ± 2.6	19.30	64.30
Vitisin B	0.9973 ± 0.0013	104.3 ± 7.4	3.0 ± 1.7	2.10	7.10
Malvidin-ethyl-catechin	0.9988 ± 0.0012	101.6 ± 3.7	4.8 ± 3.3	0.30	0.90

between 46.5 and 54.9 % of total anthocyanins in all the samples.

Additionally, the concentrations of ageing polyphenols markers were lower than those of native polyphenols in the initial wines. The concentrations of pigments linked by an ethylidene bridge (malvidin-ethylcatechin isomers) were in accordance with previous research (Blanco-Vega et al., 2014) and ranged from 0.9 to 1.75 mg.L<sup>-1</sup>. Similarly, the concentrations of pyranoanthocyanins (vitisin type A and B) in the initial wines right after bottling ranged from 0.27 to 1.1 mg.L<sup>-1</sup>, consistent with the literature (Blanco-Vega et al., 2014). Finally, concerning the concentrations of epicatechin-SO<sub>3</sub>H, they ranged from 0.40 to 0.92 mg/L and were close to the values found in young red wines by Arapitsas et al. (Arapitsas et al., 2018).

### 3.4. Evolution of native and ageing polyphenol markers during bottle storage

In order to study the overall polyphenolic concentration evolution kinetics (t<sub>0</sub>, t<sub>6</sub>, t<sub>12</sub> and t<sub>24</sub>) as a function of the red wine matrix and not the variability associated with the cork stopper, this section will be based only on the results for the D1 stopper (all experiments performed in biological replicates with triplicates for each analysis). All the kinetic curves shown in Fig. 1 are based on the normalised percent changes of each molecule with t<sub>0</sub> = 100 % for the native compounds and t<sub>0</sub> = 0 % for the ageing markers to observe the percentages of decrease and increase in comparison with the initial concentration at bottling. All the raw concentrations of each compound are given in table S6 and S7

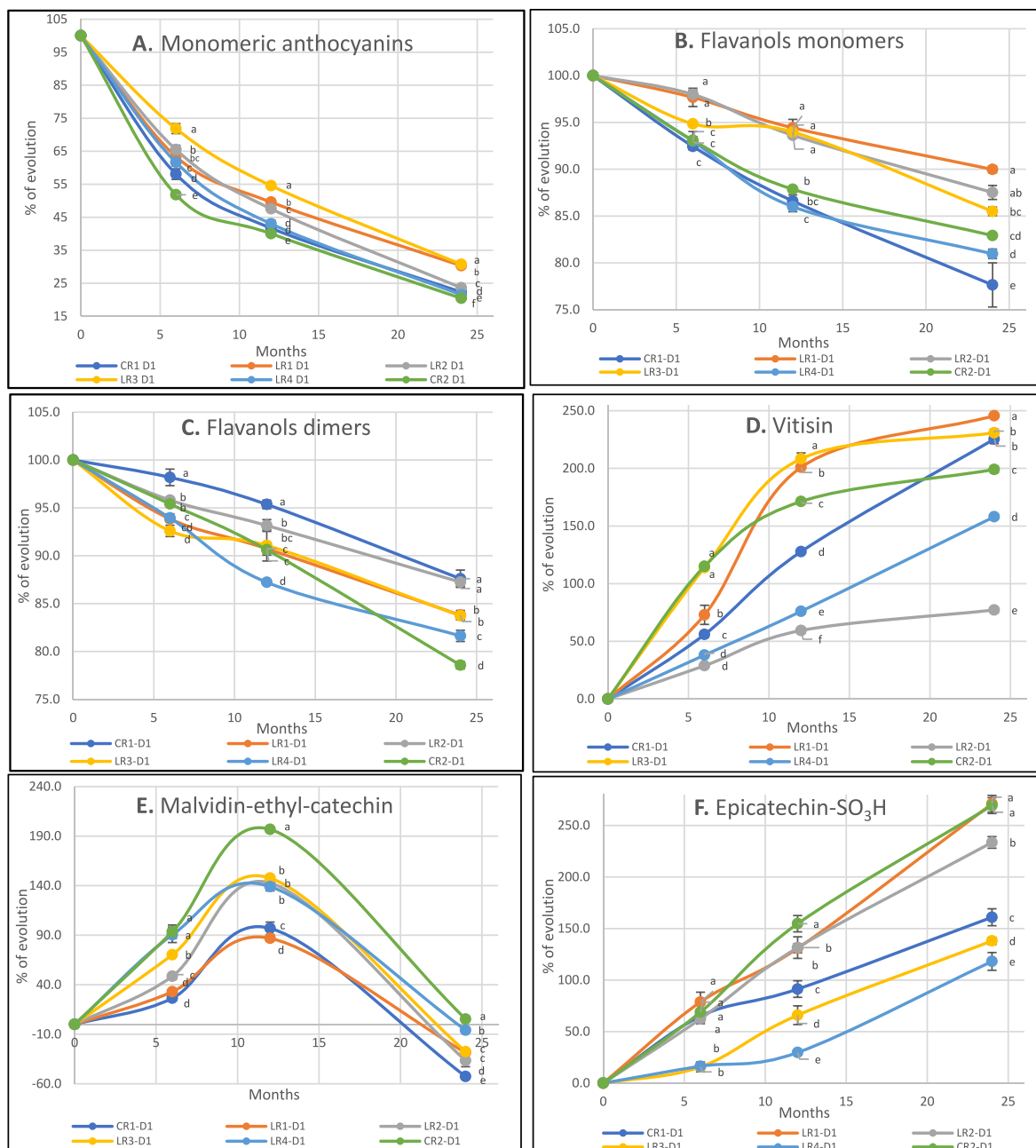


**Fig. 1.** Normalized percentage of evolution kinetics curve over 24 months of native phenolics (t<sub>0</sub> = 100 %) and ageing markers (t<sub>0</sub> = 0 %). A: sum of monomeric anthocyanins; B: sum of flavanols monomers (catechin, epicatechin, epicatechin-3-O-gallate, epigallocatechin); C: sum of flavanols dimers (B1, B2, B3, B4); D: sum of vitisin type pigment (type A, type B); E: sum of malvidin-ethyl-catechin pigment (2 isomers), F: epicatechin-SO<sub>3</sub>H. Values represent means of triplicate biological determination ± Standard Deviation. Different letters indicate the significant differences between samples in one column according to Tukey's test, p < 0.05.



(Supplementary data).

Anthocyanins, the primary pigments found in red grapes, are responsible for the color of young red wine. As depicted in Fig. 1.A., the overall monomeric pigments content showed major change during the two years of bottle ageing. The most significant alteration was observed in the reduction of original grape anthocyanins. This decrease was likely due to the formation of new pigments, particularly malvidin-3-glucoside derivatives. Despite this change, there was no notable difference in the evolution profile depending on the wine studied, with the kinetics similar to a first-order reaction with a decreasing exponential pattern in accordance with previous research (Rogez et al., 2012). However, the extent of evolution varied among different wines after 24 months of ageing. The decrease in initial concentration ranged from 69 % for LR3 to almost 80 % for CR2. In wine acidic media, the primary form for the anthocyanins would be the colorless carbinol. Nevertheless, due to the reactivity of wine components and the slow oxidative process they undergo, these anthocyanins evolve into more stable structures (Echave et al., 2021). Among the evolved anthocyanin pigments, those based on malvidin are predominant and contribute to the formation of new more stable pigments during ageing. Malvidin 3-glucoside serves as the most representative building block for these new pigments (Mateus et al., 2002). The formation of these newly developed pigments can be attributed to interactions with other wine molecules such as aldehydes or flavanols (condensed tannins) (Alcalde-Eon et al., 2006; Salas et al., 2004).

However, different wine types exhibited diverse trends. Indeed, the loss of native pigments and the formation of new pigments during ageing are closely related to the wine initial content of anthocyanins and compounds reacting with anthocyanins. A previous study (Gambuti et al., 2018) also emphasized the significant impact of the T/A ratio (Tannins to Anthocyanin ratio) (Table S5) on the reduction of native anthocyanins. Our experimental results support these observations as the wine with the highest percentage reduction had the highest T/A ratio (CR2). On the other hand, the wine with the lowest T/A is the one with the lowest anthocyanin decrease during bottle ageing (LR3). When examining changes in native flavanol monomers and dimers measured by UHPLC-MS/MS during the ageing process (Fig. 1.B. and C., respectively), a consistent decrease in the concentration of these compounds was observed across all wines during the 24-months bottle ageing period. However, unlike anthocyanins, the changes did not follow a possible first-order kinetic pattern. Instead, they had a linear type decreasing profile, as previously reported in the literature (Gambuti et al., 2020). Nevertheless, the decrease after 24 months was, on average, approximately four times lower than that of monomeric anthocyanins. Specifically, the percentage decrease ranged between 10 % and 22.4 % for monomeric flavanols and between 12.4 % and 21.4 % for dimeric flavanols. Both monomeric and dimeric flavanols may be involved in numerous oxidative and non-oxidative reactions substrates during bottle ageing. Previous studies illustrated the role of oxygen in the reactivity and stability of these compounds during bottle ageing. Ortho-hydroxyl groups on the B ring of flavanols promote oxidation to quinone, which then reacts with various nucleophiles to form new compounds during red wine ageing (Gambuti et al., 2018; Garcia et al., 2023). Additionally, flavanols can rapidly react with acetaldehyde, the main product of oxidation (Sheridan & Elias, 2016), and then indirectly condense with flavanol and/or anthocyanin units (Alcalde-Eon et al., 2006) to form new colored or colorless polymeric polyphenols. Similarly to the trends observed for anthocyanins, the evolution kinetics of flavanols may vary according to the specific wine studied. This variation may be attributed not only to the initial concentration of flavanols (Gambuti et al., 2018) but also to various factors related to the wine composition, such as pH and metal concentration, which can significantly impact the oxidation reactions of flavanols.

As expected, the concentration of native polyphenols in grapes decreases during ageing, yielding new compounds that can be described as polyphenols markers of ageing.

Indeed, vitisin A and B representing the pyranoanthocyanins, malvidin-3-O-glu-ethyl-catechin representing the ethyl-bridged polymerised pigments and epicatechin-SO<sub>3</sub>H representing the flavanol sulfonate compounds, were formed and different evolution kinetics were observed.

Through the UHPLC-MS/MS developed method, we monitored the evolution of vitisin A and B pyranoanthocyanins during the 24 months bottle ageing process (Fig. 1.D.). Vitisin pyranoanthocyanins, derived from the malvidin-3-O-glucoside and acetaldehyde or pyruvic acid, were recognized as important contributors to the color and sensory attributes of aged red wines (Echave et al., 2021; Mateus et al., 2001; Oliveira et al., 2009). Our results revealed a significant and constant increase in the concentration of these compounds during the first 12 months of ageing of the red wine samples and gradually tending towards a plateau after 24 months of ageing. A similar pattern was observed in previous studies (Wirth et al., 2010). This phenomenon sheds light on the dynamic chemical transformations occurring during wine ageing. The plateau observed in the study may be attributed to the gradual reactivity of vitisin-type pigments towards the formation of new compounds. Pyranoanthocyanins present in the wine could indeed serve as precursors for the creation of novel pigments like portisins or oxovitisins, as proposed by J. He et al. (He et al., 2010). The evolution of these compounds will vary according to the type of wine as seen for the native grape polyphenols. The evolution percentage ranged from + 77.2 % compared to the initial concentration for LR2 to + 245.6 % value for LR1. Interestingly, it was worth noting that the wines with the lowest initial concentrations after bottling exhibited the highest percentage increases. These polyphenols can be useful early ageing indicators for young red wines.

During the 24-months ageing period, the evolution of malvidin-ethyl-catechin exhibited a remarkably distinct pattern compared to other markers (Fig. 1.E.). Initially, there was a clear and significant increase in its percentage change over the first 12 months, but this trend reversed, leading to concentrations below the levels present at the time of bottling after 24 months. The significant decrease in these particular pigments in the wine may be attributed to their inherent instability when compared to pyranoanthocyanins. Anthocyanin-ethyl-flavanol pigments have a relatively lower stability in aqueous environments and are prone to undergoing cleavage, resulting in the formation of a vinylflavanol (Mateus et al., 2002).

This newly formed vinylflavanol can subsequently interact with an anthocyanin, leading to the creation of an orange-colored flavanol-pyranoanthocyanin. This process also provides a partial explanation to the shift towards an orange-red tint for the color of "old" red wines (Alcalde-Eon et al., 2006). At their maximum of concentration, at around 12 months, the percentage of evolution varied from one wine to another. The range spanned from + 86.9 % for LR1 to + 196.8 % for CR2. These differences could potentially be influenced by the initial free SO<sub>2</sub> levels present in the wines. The free SO<sub>2</sub> content plays a role in modulating the amount of acetaldehyde that forms in the bottle during the oxidation of ethanol. In our study, even though the free SO<sub>2</sub> concentration was adjusted to 30 mg.L<sup>-1</sup> before bottling for all wines, the concentration measured shortly after bottling slightly differed between CR2 (25 mg.L<sup>-1</sup>) and LR1 (30.7 mg.L<sup>-1</sup>). In summary, the evolution of malvidin-ethyl-catechin during the 24-month ageing period showed a unique pattern, likely influenced by the inherent instability of its structure and its propensity to undergo reactions that contribute to the characteristic color transformation seen in aged red wines.

Pyranoanthocyanins and ethyl-bonded pigments belong to two metabolite families formed through acetaldehyde-polyphenols reactions. However, the last ageing marker studied, epicatechin-SO<sub>3</sub>H, follows a different formation pathway as it arises essentially from the acid depolymerization of tannin oligomers and polymers. This marker accumulates gradually and continually throughout the ageing process due to the reaction between flavanols and sulfites present in the wine. This result in the formation of a 4β-sulfonate adduct on the C ring of the

flavanol (Arapitsas et al., 2014; Ma et al., 2018).

There is a consistent and linear evolution type in the concentration of this marker regardless of the wine studied (Fig. 1.F). This pattern is in accordance with findings in the literature (Arapitsas et al., 2014). Like the other compounds, the rate of change in concentration depends on the wine involved. After 24 months of ageing, the percentage increase compared to the initial concentration ranged from + 118.1 % for LR4 to + 271.1 % for LR1. These differences might be influenced by storage conditions like temperature (Arapitsas et al., 2014). In our study, we maintained standardized storage conditions at 17 °C, thereby eliminating temperature as a contributing factor in the evolution of the analyzed wines.

Throughout the 24 months ageing period, significant changes were

observed in the native polyphenols and ageing markers. Depending on the molecule, the kinetics of evolution follow different patterns. The wine type or matrix studied may impact this evolution by increasing or slowing down the rate of evolution during red wine ageing.

### 3.5. Influence of cork OTR on the evolution of polyphenols

As observed in the previous section, the overall evolution of the targeted polyphenols during 24 months varied depending on the molecule being analyzed and the type of red wine studied. However, it is essential to also consider the influence of the cork stopper on these evolution profiles, especially for the changes attributed to oxidative mechanisms. Because of its physical properties, the cork is going to bring

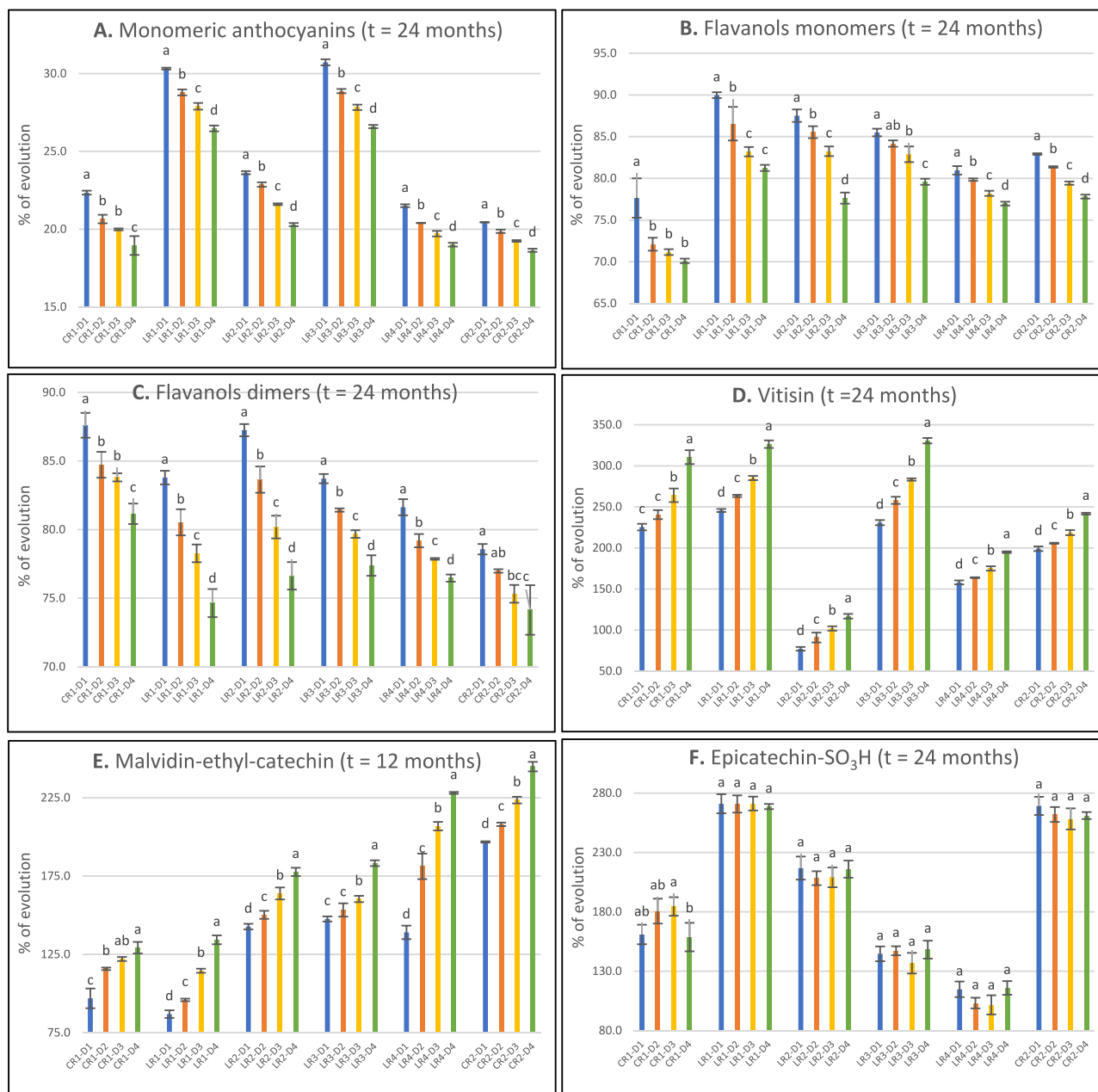


**Fig. 2.** Normalized percentage of evolution at 12 or 24 months of native phenolics ( $t_0 = 100\%$ ) and ageing markers ( $t_0 = 0\%$ ) for each wine/cork combination. A: sum of monomeric anthocyanins; B: sum of flavanols monomers (catechin, epicatechin, epicatechin-3-O-gallate, epigallocatechin); C: sum of flavanols dimers (B1, B2, B3, B4); D: sum of vitisin type pigment (type A, type B); E: sum of malvidin-ethyl-catechin pigment (2 isomers), F: epicatechin-SO<sub>3</sub>H. Values represent means of triplicate biological determination  $\pm$  Standard Deviation. Different letters indicate the significant differences between samples in one column according to Tukey's test,  $p < 0.05$ .

oxygen to the wine throughout bottle ageing and this oxygen transfer rate (OTR) becomes a crucial parameter that may influence the wine shelf life (Pons et al., 2022). For this study, the wines were bottled using four micro-agglomerated corks with different OTRs, referred to as D1, D2, D3 and D4, with their respective characteristics provided in Table 1.

One of our goals was to compare the differences in the evolution of specific polyphenol molecules in relation with stopper used after 24 months of ageing. Fig. 2 illustrates the change as a % of initial concentration for each wine/stopper combination for each family of compounds at 12 or 24 months. When examining the influence of OTR on the evolution of monomeric anthocyanins (Fig. 2.A.), a noticeable reduction in total monomeric anthocyanins was evident over time and with increasing OTR after 24 months, regardless of the specific wine sample under study.

This observation was in accordance with findings reported in the literature (Gambuti et al., 2013; Wirth et al., 2010, 2012). Notably, the two wine samples LR4 and CR2 exhibited similar trends. The difference of evolution percentage ( $\Delta E\%$ ) between the two extreme cork types (D1 and D4) for a given ageing time ( $t = 12$  or 24 months), varied from 1.8 % for CR2 to 4.1 % for LR3. This consistent trend was observed for all three types of anthocyanins naturally found in grapes, namely monoglucoside, acetyl glucoside, and coumaroyl glucoside anthocyanins. Indeed, the rise in OTR promoted the involvement of these molecules in oxygen-activated reactions between anthocyanins and flavanols such as pyranoanthocyanins and ethyl-linked pigment formation.

We observed a similar influence of OTR as seen with monomeric anthocyanins for the native flavanol monomers and dimers (Fig. 2.B. and C., respectively) after 24 months of bottle ageing. Notably, there is a significant decrease in the percentage of evolution for these two flavanol families. With a  $\Delta E\%$  for flavanol monomers ranging from 4.0 % for LR4 to 9.9 % for LR2, and between 4.4 % (CR2) to 10.6 % (LR2) for flavanol dimers. These findings are in accordance with previous research (Gambuti et al., 2013; Wirth et al., 2010) which also demonstrated a noteworthy effect of increasing OTR on the reduction of low molecular weight polyphenols. This phenomenon can be explained by the reactivity of these compounds to form reactive quinones. These quinones can undergo scavenging reactions with other nucleophiles, such as flavanols, aromatic compounds,  $\text{SO}_2$ , and others molecules. In addition, indirect oxidation reactions mediated by acetaldehyde play a role, promoting the formation of polymeric polyphenols involving flavanols to form both pigmented and non-pigmented polyphenols (Alcalde-Eon et al., 2006; Sheridan & Elias, 2016).

In general, higher cork oxygen transfer rates (OTRs) resulted in a decrease in native polyphenols over the course of red wine bottle ageing. The difference in oxygen supply through the cork therefore promoted an increase in ageing markers caused by red wine oxidation.

The percentage of evolution of vitisins (A and B) pigments over 24 months for each wine/cork combination (Fig. 2.D.) had an opposite trend compared to the native compounds. Indeed, there was a significant increase of those compounds as the OTR of the cork increased. These findings aligned with those of previous studies (Wirth et al., 2010, 2012). The  $\Delta E\%$  values varied from 36.8 % for LR4 to 99.8 % for LR3, showing the critical role of stopper type in the formation of these compounds. Consequently, higher OTR lead to an enhanced supply of oxygen to the wine and the formation of acetaldehyde, thus facilitating the oxidative transformation of anthocyanins into pyranoanthocyanins. Consequently, the concentration of pyranoanthocyanins tends to steadily increase during the early stages of ageing.

Another group of oxidation markers, namely the ethyl-linked pigments were investigated by following malvidin-ethyl-catechin. As demonstrated in section 3.4., this marker served as an early indicator of red wine ageing, exhibiting an initial increase over the first 12 months, followed by a subsequent decrease throughout the time. Hence, to investigate the impact of the cork OTR in the initial months of wine ageing, the evolution percentages was compared at the point of maximum accumulation at 12 months rather than 24 months (Fig. 2.E.).

Similar to the vitisin pigments, the trend was similar for all the wines with an augmentation of malvidin-ethyl-catechin as cork OTR increased. This change in percentage when comparing corks ( $\Delta E\%$ ) varied from 32.3 % for CR1 to 89.1 % for LR4. The higher cork OTR facilitated the oxidative transformation of anthocyanins into ethyl-linked pigments through the formation of acetaldehyde (Giuffrida de Esteban et al., 2019). This phenomenon led to a steady increase in the concentration of ethyl-linked pigments during the early stages of wine ageing.

Lastly, we studied the impact of the cork oxygen transfer rate on the evolution of epicatechin- $\text{SO}_3\text{H}$  (Fig. 2.F.). We observed that there was no significant difference in the evolution of this compound among the different corks for all the analyzed wines. This suggests that the formation of flavanol sulfonates was not influenced by the OTR of the cork stopper. Unlike the other polyphenolic compounds studied *i.e.* pyranoanthocyanins and ethyl-linked pigments, which undergo oxidative reactions during wine ageing, flavanol sulfonates are formed through a different chemical mechanism. Specifically, they are produced via the acid-catalyzed depolymerization of tannin oligomers and polymers followed by the nucleophilic addition of sulfonate (Ma et al., 2018). As a result, the oxygen transfer rate (OTR) of the cork, does not play a substantial role in the formation of flavanol sulfonates. Instead, the concentration of flavanol sulfonates accumulates gradually during the ageing process (Arapitsas et al., 2014, 2018) as shown in part 3.4. The formation of flavanol sulfonates appears then to be largely independent of the presence of oxygen and is driven primarily by other chemical interactions in the wine matrix.

These results demonstrated that the cork oxygen transfer rate (OTR) played a critical role in influencing the evolution of some polyphenols in wine. Higher OTR promoted a reduction in native polyphenols, such as anthocyanins and flavanols, during the ageing process, as these compounds were more susceptible to oxidative reactions mediated by acetaldehyde and quinone formation. Vitisins pigments and ethyl-linked pigments increased with increasing cork OTR, indicative of their involvement in oxygen-activated reactions. However, the formation of flavanol sulfonates was found to be independent of the OTR, as these compounds are produced through non-oxidative mechanisms involving sulfites and flavanols.

#### 4. Conclusion

This study investigated the evolution of native and ageing marker polyphenols during 24 months of bottled red wines and the influence of cork oxygen transfer rate (OTR) on these transformations. Anthocyanins, the primary pigments in red grapes, underwent significant changes during the ageing process, with a decrease in original grape anthocyanins and the formation of new pigments, particularly malvidin-3-glucoside derivatives. Flavanols also exhibited a linear decrease in concentration, showing their reactivity in various oxidative and non-oxidative reactions. In contrast, the formation of pyranoanthocyanins, ethyl-linked pigments and flavanol sulfonates had distinct patterns during ageing. The cork OTR played a crucial role in influencing the evolution of polyphenols, as higher OTR led to decrease native polyphenols, increase vitisin pigments and ethyl-linked pigments, but had no significant impact on the formation of flavanol sulfonates. This study provided then valuable insights into the chemical transformations occurring during wine ageing and emphasized the importance of cork stopper selection in preserving wine quality over time. Further research in this area can contribute to optimize wine ageing processes and enhance the understanding of the factors that are involved in the evolution of polyphenols in wine.

#### CRedit authorship contribution statement

**Luca Garcia:** Investigation, Methodology, Writing – original draft, Writing – review & editing, Formal analysis. **Elodie Martet:** Formal analysis. **Lucas Suc:** Methodology, Formal analysis, Writing – review &

editing. **François Garcia:** Methodology, Supervision, Writing – review & editing. **Cédric Saucier:** Conceptualization, Funding acquisition, Methodology, Project administration, Supervision, Writing – review & editing.

### Declaration of competing interest

The authors declare that they have no known competing financial interests or personal relationships that could have appeared to influence the work reported in this paper.

### Data availability

Data will be made available on request.

### Acknowledgements

We acknowledged Diam bouchage company for funding this project and PhD grant of Luca Garcia from University of Montpellier (UM200893). Winemakers from Languedoc-Roussillon and Côtes du Rhône are thanked for allowing sampling in their cellars. Vivelys is acknowledged for its help in wine bottling. Dr Christine Le Guernevé is thanked for her help for NMR analysis.

### Appendix A. Supplementary material

Supplementary data to this article can be found online at <https://doi.org/10.1016/j.foodchem.2024.138491>.

### References

- Alcalde-Eon, C., Escribano-Bailón, M. T., Santos-Buelga, C., & Rivas-Gonzalo, J. C. (2006). Changes in the detailed pigment composition of red wine during maturity and ageing : A comprehensive study. *Analytica Chimica Acta*, 563(1), 238–254. <https://doi.org/10.1016/j.aca.2005.11.028>
- Arapitsas, P., Guella, G., & Mattivi, F. (2018). The impact of SO<sub>2</sub> on wine flavanols and indoles in relation to wine style and age. *Scientific Reports*, 8(1), Article 1. <https://doi.org/10.1038/s41598-018-19185-5>
- Arapitsas, P., Speri, G., Angeli, A., Perenzoni, D., & Mattivi, F. (2014). The influence of storage on the “chemical age” of red wines. *Metabolomics*, 10(5), 816–832. <https://doi.org/10.1007/s11306-014-0638-x>
- Bakker, J., & Timberlake, C. F. (1997). Isolation, Identification, and Characterization of New Color-Stable Anthocyanins Occurring in Some Red Wines. *Journal of Agricultural and Food Chemistry*, 45(1), 35–43. <https://doi.org/10.1021/jf960252c>
- Blanco-Vega, D., Gómez-Alonso, S., & Hermosín-Gutiérrez, I. (2014). Identification, content and distribution of anthocyanins and low molecular weight anthocyanin-derived pigments in Spanish commercial red wines. *Food Chemistry*, 158, 449–458. <https://doi.org/10.1016/j.foodchem.2014.02.154>
- Boulton, R. B. (2005). *The physics of wine bottle closures*. Seattle, WA: The Science of Closures Seminar.
- de Freitas, V., & Mateus, N. (2011). Formation of pyranoanthocyanins in red wines : A new and diverse class of anthocyanin derivatives. *Analytical and Bioanalytical Chemistry*, 401(5), 1463–1473. <https://doi.org/10.1007/s00216-010-4479-9>
- Echave, J., Barral, M., Fraga-Corral, M., Prieto, M. A., & Simal-Gandara, J. (2021). Bottle Aging and Storage of Wines : A Review. *Molecules*, 26(3), Article 3. <https://doi.org/10.3390/molecules26030713>
- Escribano-Bailón, T., Álvarez-García, M., Rivas-Gonzalo, J. C., Heredia, F. J., & Santos-Buelga, C. (2001). Color and Stability of Pigments Derived from the Acetaldehyde-Mediated Condensation between Malvidin 3-O-Glucoside and (+)-Catechin. *Journal of Agricultural and Food Chemistry*, 49(3), 1213–1217. <https://doi.org/10.1021/jf0010811>
- Fulcrand, H., Dueñas, M., Salas, E., & Cheynier, V. (2006). Phenolic Reactions during Winemaking and Aging. *American Journal of Enology and Viticulture*, 57(3), 289–297. <https://doi.org/10.5344/ajev.2006.57.3.289>
- Gambuti, A., Picariello, L., Rinaldi, A., & Moio, L. (2018). Evolution of Sangiovese Wines With Varied Tannin and Anthocyanin Ratios During Oxidative Aging. *Frontiers in Chemistry*, 6. <https://www.frontiersin.org/articles/10.3389/fchem.2018.00063>
- Gambuti, A., Picariello, L., Rinaldi, A., Ugliano, M., & Moio, L. (2020). Impact of 5-year bottle aging under controlled oxygen exposure on sulfur dioxide and phenolic composition of tannin-rich red wines. *OENO One*, 54(3), Article 3. <https://doi.org/10.20870/oeno-one.2020.54.3.3527>
- Gambuti, A., Rinaldi, A., Ugliano, M., & Moio, L. (2013). Evolution of Phenolic Compounds and Astringency during Aging of Red Wine : Effect of Oxygen Exposure before and after Bottling. *Journal of Agricultural and Food Chemistry*, 61(8), 1618–1627. <https://doi.org/10.1021/jf302822b>
- García, L., Deshaies, S., Constantin, T., García, F., & Saucier, C. (2023). Impact of phenolic composition and antioxidant parameters on the ageing potential of Syrah red wines measured by accelerated ageing tests. *Food Chemistry*, 426, Article 136613. <https://doi.org/10.1016/j.foodchem.2023.136613>
- García-Beneytez, E., Cabello, F., & Revilla, E. (2003). Analysis of Grape and Wine Anthocyanins by HPLC-MS. *Journal of Agricultural and Food Chemistry*, 51(19), 5622–5629. <https://doi.org/10.1021/jf0302207>
- Giuffrida de Esteban, M. L., Ubeda, C., Heredia, F. J., Catania, A. A., Assof, M. V., Fanzone, M. L., & Jofre, V. P. (2019). Impact of closure type and storage temperature on chemical and sensory composition of Malbec wines (Mendoza, Argentina) during aging in bottle. *Food Research International*, 125, Article 108553. <https://doi.org/10.1016/j.foodres.2019.108553>
- He, J., Oliveira, J., Silva, A. M. S., Mateus, N., & De Freitas, V. (2010). Oxovitisins : A New Class of Neutral Pyranone-anthocyanin Derivatives in Red Wines. *Journal of Agricultural and Food Chemistry*, 58(15), 8814–8819. <https://doi.org/10.1021/jf101408q>
- Jackson, M. G., Timberlake, C. F., Bridle, P., & Vallis, L. (1978). Red wine quality : Correlations between colour, aroma and flavour and pigment and other parameters of young Beaujolais. *Journal of the Science of Food and Agriculture*, 29(8), 715–727. <https://doi.org/10.1002/jsfa.2740290810>
- Lambert, M., Meudec, E., Verbaere, A., Mazerolles, G., Wirth, J., Masson, G., Cheynier, V., & Sommerer, N. (2015). A High-Throughput UHPLC-QqQ-MS Method for Polyphenol Profiling in Rosé Wines. *Molecules*, 20(5), Article 5. <https://doi.org/10.3390/molecules20057890>
- Landraut, N., Poucheret, P., Ravel, P., Gasc, F., Cros, G., & Teissedre, P.-L. (2001). Antioxidant Capacities and Phenolics Levels of French Wines from Different Varieties and Vintages. *Journal of Agricultural and Food Chemistry*, 49(7), 3341–3348. <https://doi.org/10.1021/jf010128f>
- Ma, L., Watrelot, A. A., Addison, B., & Waterhouse, A. L. (2018). Condensed Tannin Reacts with SO<sub>2</sub> during Wine Aging, Yielding Flavan-3-ol Sulfonates. *Journal of Agricultural and Food Chemistry*, 66(35), 9259–9268. <https://doi.org/10.1021/acs.jafc.8b01996>
- Mateus, N., Silva, A. M. S., Santos-Buelga, C., Rivas-Gonzalo, J. C., & de Freitas, V. (2002). Identification of Anthocyanin-Flavanol Pigments in Red Wines by NMR and Mass Spectrometry. *Journal of Agricultural and Food Chemistry*, 50(7), 2110–2116. <https://doi.org/10.1021/jf0111561>
- Mateus, N., Silva, A. M. S., Vercauteren, J., & de Freitas, V. (2001). Occurrence of Anthocyanin-Derived Pigments in Red Wines. *Journal of Agricultural and Food Chemistry*, 49(10), 4836–4840. <https://doi.org/10.1021/jf001505b>
- Oliveira, J., de Freitas, V., & Mateus, N. (2009). A novel synthetic pathway to vitisin B compounds. *Tetrahedron Letters*, 50(27), 3933–3935. <https://doi.org/10.1016/j.tetlet.2009.04.072>
- Pissarra, J., Lourenço, S., González-Paramás, A. M., Mateus, N., Santos Buelga, C., Silva, A. M. S., & De Freitas, V. (2005). Isolation and structural characterization of new anthocyanin-alkyl-catechin pigments. *Food Chemistry*, 90(1), 81–87. <https://doi.org/10.1016/j.foodchem.2004.03.027>
- Pons, A., Lavigne, V., Suhas, E., Thibon, C., Redon, P., Loisel, C., & Darriet, P. (2022). Impact of the Closure Oxygen Transfer Rate on Volatile Compound Composition and Oxidation Aroma Intensity of Merlot and Cabernet Sauvignon Blend : A 10 Year Study. *Journal of Agricultural and Food Chemistry*, 70(51), 16358–16368. <https://doi.org/10.1021/acs.jafc.2c07475>
- Quaglieri, C., Prieto-Perea, N., Berrueta, L. A., Gallo, B., Rasines-Perea, Z., Jourdes, M., & Teissedre, P.-L. (2017). Comparison of Aquitaine and Rioja Red Wines. In *Characterization of Their Phenolic Composition and Evolution from 2000 to 2013*. <https://doi.org/10.3390/molecules22020192>
- Revilla, E., García-Beneytez, E., Cabello, F., Martín-Ortega, G., & Ryan, J.-M. (2001). Value of high-performance liquid chromatographic analysis of anthocyanins in the differentiation of red grape cultivars and red wines made from them. *Journal of Chromatography A*, 915(1), 53–60. [10.1016/S0021-9673\(01\)00635-5](https://doi.org/10.1016/S0021-9673(01)00635-5)
- Ribéreau-Gayon, P., Dubourdieu, D., Donèche, B., & Lonvaud, A. (1998). *Traité d'oenologie : Microbiologie du vin, vinifications*. Dunod.
- Rogez, H., Akwie, S. N. L. T., Moura, F. G., & Larondelle, Y. (2012). Kinetic Modeling of Anthocyanin Degradation and Microorganism Growth during Postharvest Storage of Açai Fruits (Euterpe oleracea). *Journal of Food Science*, 77(12), C1300–C1306. <https://doi.org/10.1111/j.1750-3841.2012.02996.x>
- Roland, A., & Schneider, R. (2015). Development and validation of a high-throughput analysis of glutathione in grapes, musts and wines by Stable Isotope Dilution Assay and LC-MS/MS. *Food Chemistry*, 177, 152–157. <https://doi.org/10.1016/j.foodchem.2015.01.027>
- Salas, E., Atanasova, V., Poncet-Legrand, C., Meudec, E., Mazauric, J. P., & Cheynier, V. (2004). Demonstration of the occurrence of flavanol-anthocyanin adducts in wine and in model solutions. *Analytica Chimica Acta*, 513(1), 325–332. <https://doi.org/10.1016/j.aca.2003.11.084>
- Sheridan, M. K., & Elias, R. J. (2016). Reaction of Acetaldehyde with Wine Flavonoids in the Presence of Sulfur Dioxide. *Journal of Agricultural and Food Chemistry*, 64(45), 8615–8624. <https://doi.org/10.1021/acs.jafc.6b03565>
- Somers, T. C. (1971). The polymeric nature of wine pigments. *Phytochemistry*, 10(9), 2175–2186. [https://doi.org/10.1016/S0031-9422\(00\)97215-7](https://doi.org/10.1016/S0031-9422(00)97215-7)
- Tao, Y., García, J. F., & Sun, D.-W. (2014). Advances in Wine Aging Technologies for Enhancing Wine Quality and Accelerating Wine Aging Process. *Critical Reviews in Food Science and Nutrition*, 54(6), 817–835. <https://doi.org/10.1080/10408398.2011.609949>
- Tománková, E., Balík, J., Soural, I., Bednář, P., & Papoušková, B. (2016). Colour and antioxidant properties of malvidin-3-glucoside and Vitisin A. *Acta Alimentaria*, 45(1), 85–92. <https://doi.org/10.1556/066.2016.45.1.11>
- Vidal, S., Francis, L., Noble, A., Kwiatkowski, M., Cheynier, V., & Waters, E. (2004). Taste and mouth-feel properties of different types of tannin-like polyphenolic compounds



- and anthocyanins in wine. *Analytica Chimica Acta*, 513(1), 57–65. <https://doi.org/10.1016/j.aca.2003.10.017>
- Wildenrad, H. L., & Singleton, V. L. (1974). The Production of Aldehydes as a Result of Oxidation of Polyphenolic Compounds and its Relation to Wine Aging. *American Journal of Enology and Viticulture*, 25(2), 119–126.
- Wirth, J., Caillé, S., Souquet, J. M., Samson, A., Dieval, J. B., Vidal, S., Fulcrand, H., & Cheynier, V. (2012). Impact of post-bottling oxygen exposure on the sensory characteristics and phenolic composition of Grenache rosé wines. *Food Chemistry*, 132(4), 1861–1871. <https://doi.org/10.1016/j.foodchem.2011.12.019>
- Wirth, J., Morel-Salmi, C., Souquet, J. M., Dieval, J. B., Aagaard, O., Vidal, S., Fulcrand, H., & Cheynier, V. (2010). The impact of oxygen exposure before and after bottling on the polyphenolic composition of red wines. *Food Chemistry*, 123(1), 107–116. <https://doi.org/10.1016/j.foodchem.2010.04.008>